

## COMPARING MICROWAVE DETECTED PHOTOCONDUCTANCE, QUASI STEADY STATE PHOTOCONDUCTANCE AND PHOTOLUMINESCENCE IMAGING FOR IRON ANALYSIS IN SILICON

M. Pengerla<sup>\*1</sup>, S. Al-Hajjawi<sup>1</sup>, V. Kuruganti<sup>1</sup>, J. Haunschild<sup>1</sup>, N. Schüler<sup>2</sup>, K. Dornich<sup>2</sup>, S. Rein<sup>1</sup>

<sup>1</sup>Fraunhofer Institute for Solar Energy Systems ISE, Heidenhofstraße 2, 79110 Freiburg, Germany

<sup>2</sup>Freiberg Instruments GmbH, Delfter Str. 6, 09599, Freiberg, Germany

\*Telephone: +49 761 4588 5644, e-mail: monica.pengerla@ise.fraunhofer.de

**ABSTRACT:** Interstitial iron (Fe<sub>i</sub>) is one of the most prominent metallic impurities in crystalline silicon, as it is fast diffusive and highly recombination-active. Its accurate detection is crucial for quality control during solar cell production as iron contamination can significantly limit solar cell efficiency. This work gives a qualitative and quantitative comparison of iron characterization tools including QSSPC (quasi steady state photoconductance), PLI (Photoluminescence Imaging) and MDP (Microwave detected photo conductance). The detection limits, feasibility and accuracy of each tool for iron detection are investigated. In principle, despite of different injection regimes, the absolute iron concentration measured on the different characterising tools is in the same order of magnitude with very good qualitative and quantitative correlation. With the results obtained, the comparison of QSSPC, PLI and MDP showed a mean deviation of 20%.

**Keywords:** Silicon, Lifetime, Iron concentration, MDP map

### 1 INTRODUCTION

In silicon wafers used in PV industry, metallic impurities like Fe, Cr, Ni and Cu are present and may exceed concentrations of  $10^{12}$  at/cm<sup>3</sup> [1]. Among the transition metals, iron has the highest solubility of  $8.4 \cdot 10^{25}$  at/cm<sup>3</sup> [2] in the silicon lattice and is one of the fastest diffusing species with a rate of  $1.3 \cdot 10^{-3}$  cm<sup>2</sup>/s [3]. Iron impurities enter silicon wafers from the feedstock, from the crucible, or during various processing steps [4].

The strong injection-dependent recombination nature of iron has a weak influence on  $V_{oc}$  but has a significant impact on  $J_{sc}$ , MPP and Fill factor [5]. Interstitial iron (Fe<sub>i</sub>) can partially be gettering during emitter diffusion but still limits efficiency. To understand Fe behaviour, spatially resolved accurate Fe distribution information in wafers at every stage of production plays a prominent role for process optimization. Therefore, characterizing tools accuracy, measuring conditions, correlation between different tools and an easy procedure becomes crucial for Fe detection.

For iron evaluation in QSSPC, we use a Sinton Instruments WTC-120. For PLI, we use the PL modulium setup developed by Fraunhofer ISE [8], which has a feature for automatic iron analysis. For MDP, we use a MDPmap device from Freiberg Instruments which also has an automatic procedure implemented.

The goal of this paper is to look into the following topics:

- Lifetime and injection values play a crucial role for iron detection. To estimate the accuracy of lifetime and injection evaluation of MDP, PL and QSSPC injection-dependent lifetime curves of these tools are correlated.
- Spatial qualitative and quantitative iron concentration comparison between PLI and MDP are performed to check the difference in iron concentration, considering PLI as reference. Obtained Fe<sub>i</sub> maps from MDP and PLI are compared to QSSPC by averaging few centimetres in the centre region of the wafer.
- Find optimal measurement conditions for a good correlation (same order of magnitude) in the three tools.

If there exist discrepancies, then investigation of reasons.  
d) The detection limits, feasibility and accuracy of each tool for iron detection are investigated.

### 2 EXPERIMENTAL DETAILS

#### 2.1 SAMPLE SET

sample	Sample type	Thickness (μm)	resistivity (Ωcm)	Surface passivation
01	mc	200	1.28	Al <sub>2</sub> O <sub>3</sub>
02	mc	200	1.02	Al <sub>2</sub> O <sub>3</sub>
03	mc	200	1.18	SiN <sub>x</sub>
04	mc	200	1.03	SiN <sub>x</sub>
05	mc	200	0.93	SiN <sub>x</sub>
06	FZ	502	2.7	Al <sub>2</sub> O <sub>3</sub>
07	FZ	503	2.7	Al <sub>2</sub> O <sub>3</sub>

The sample set used for the tool comparison consists of 5 multi-crystalline (mc-Si) and 2 float zone (FZ) samples with intentional iron contamination. By storing samples in a black box for two days in the dark, the available iron is fully transformed into the FeB state.

#### 2.2 LIFETIME EVALUATION METHODS

In QSSPC, the photoconductance is recorded after a strong excitation flash and is converted to injection values. With the known generation rates, the injection-dependent charge carrier lifetimes are calculated [9]. Fig.1 represents the injection-dependent lifetime measurement on sample 01. The red, green and blue curves represent the QSSPC, PL modulium and MDP injection-dependent lifetimes.

PLI considers the measured intensity counts for transformation into injection under homogeneous laser excitation of the sample, which results in lifetime images [6]. In PL modulium for an injection dependent lifetime, the generation rate varies from 0.001 to 1.6 suns with a

measurement spot of 45mm diameter. A modulated intensity detector measures the generation rate or laser excitation intensity. Another detector, underneath the sample, detects the PL response with respect to excitation. Detailed explanation can be found in [8].

MDP extracts the lifetime by curve fitting from  $\frac{1}{4}$ <sup>th</sup> to  $\frac{3}{4}$ <sup>th</sup> part of the transient decay after excitation. The extracted lifetime is assigned to the injection, right before the laser is turned off [7]. MDP has three lasers with a wavelength of 980 nm and a laser power of 0.11, 3 and 70 mW, respectively, to cover a wide injection range. In Fig. 1. at low injections ( $1 \times 10^{11}$  to  $1 \times 10^{12} \text{cm}^{-3}$ ) deviations can be observed in MDP curve due to low signal to noise ratio. Whereas, at high injections due to skin depth effects of microwave, the lifetime measured from the logarithmic transient decay is larger than the expected lifetime [7].

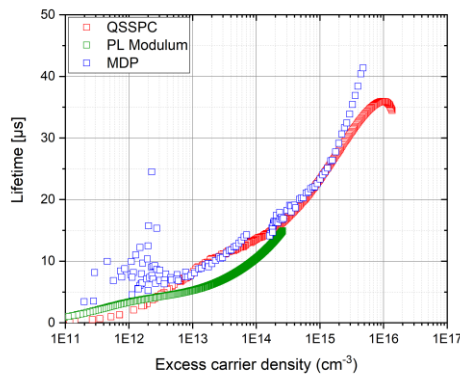


Figure 1: Injection-dependent lifetime curves measured with different techniques.

### 2.3 CALCULATION OF IRON CONCENTRATION

For the calculation of interstitial iron, the above mentioned three tools work by the approach developed by Zoth and Bergholz [10]. It explains that at room temperature in p-type silicon Fe bonds with acceptor atoms and forms Fe-B pairs. Due to the differences in the position of their energy levels within the bandgap and in the capture properties of electron holes, the injection dependence of the lifetime curve changes between the FeB and Fe<sub>i</sub> defect states. The change in lifetime before and after dissociation can be used to calculate the Fe<sub>i</sub> concentration as shown in the Equation below.  $\tau_a$ ,  $\tau_b$  are the carrier lifetimes in Fe<sub>i</sub>, FeB states and C is an injection- and doping-dependent factor [11]. The injection density where the recombination properties of both states are equal (no change in lifetime) is referred as crossover point (Fig. 2)

$$Fe_i = C \left( \frac{1}{\tau_a} - \frac{1}{\tau_b} \right)$$

A typical QSSPC injection-dependent lifetime plot is shown in Fig. 2. The injection-dependent lifetime is measured before (black curve) and after (red curve) FeB dissociation. FeB dissociation is achieved with constant laser illumination with approximately two suns intensity for two minutes. From the results, considering lifetimes at carrier injection density  $1 \times 10^{15} \text{cm}^{-3}$ , the iron concentration is calculated manually.

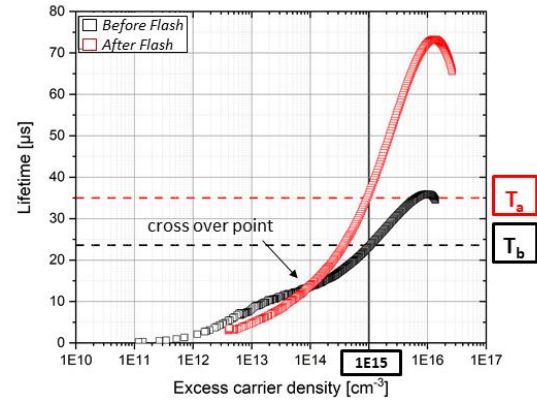


Figure 2: QSSPC based iron detection method.

In PLI the injection is maintained at approximately  $1 \times 10^{12} \text{cm}^{-3}$ , the exposure times were maintained at 120 seconds for Fe-B state and 180 seconds for Fe<sub>i</sub>. The lifetime images in FeB and Fe<sub>i</sub> state with a dissociation step of around 2.5 suns for 4 min are performed and the iron concentration image is calculated. In MDP, the lifetime mappings of FeB and Fe<sub>i</sub> and the dissociation step are performed automatically. The lifetime mapping in MDP is performed at roughly  $1 \times 10^{15} \text{cm}^{-3}$  injection with laser excitation durations in microseconds per position. The measurement time for both FeB and Fe<sub>i</sub> lifetime maps is 5min with 1mm resolution. It is also possible to go for less measurement time with lower resolutions. For dissociation in MDP a 3000 W flash lamp is part of the setup. The QSSPC and PLI apply the Macdonald-Istratov defect model [12,4], whereas MDP adapted the S. Rein and S. Glunz defect model [11].

The obtained Fe<sub>i</sub> map from MDP and PLI is compared to QSSPC by averaging few centimeters in the center region of the wafer. QSSPC and MDP measurements are performed at high injections (above cross over point), whereas PLI in low injections (below cross over point).

### 3 SPATIALLY RESOLVED COMPARISON

Fig. 3 illustrates a spatial comparison of iron concentration images/maps obtained by PLI and MDP. A good qualitative correlation of spatially resolved Fe concentration can be observed. The average injection value of the PL image is  $1 \times 10^{12} \text{cm}^{-3}$ . In the regions of low iron concentration the injection was below  $10^{11} \text{cm}^{-3}$ . Low signal in those injection regions makes the image noisy, which can be observed in sample 4 and sample 7 (Fig. 3d and 3g). This could be avoided by applying higher injections and less exposure times, but at high injections there could be small fraction of FeB dissociation due to the laser excitation during the measurement. The grey regions in the MDP Fe map Fig. 3i correspond to the injection regions near to cross over point. In Fig. 3e and 3l differences in qualitative comparison of center region can be observed. In comparison to QSSPC, Fig. 3e shows a factor of three difference, whereas in MDP a factor of two. This was due to the chosen high injection region in PL, due to the low PL signal in low injection region.

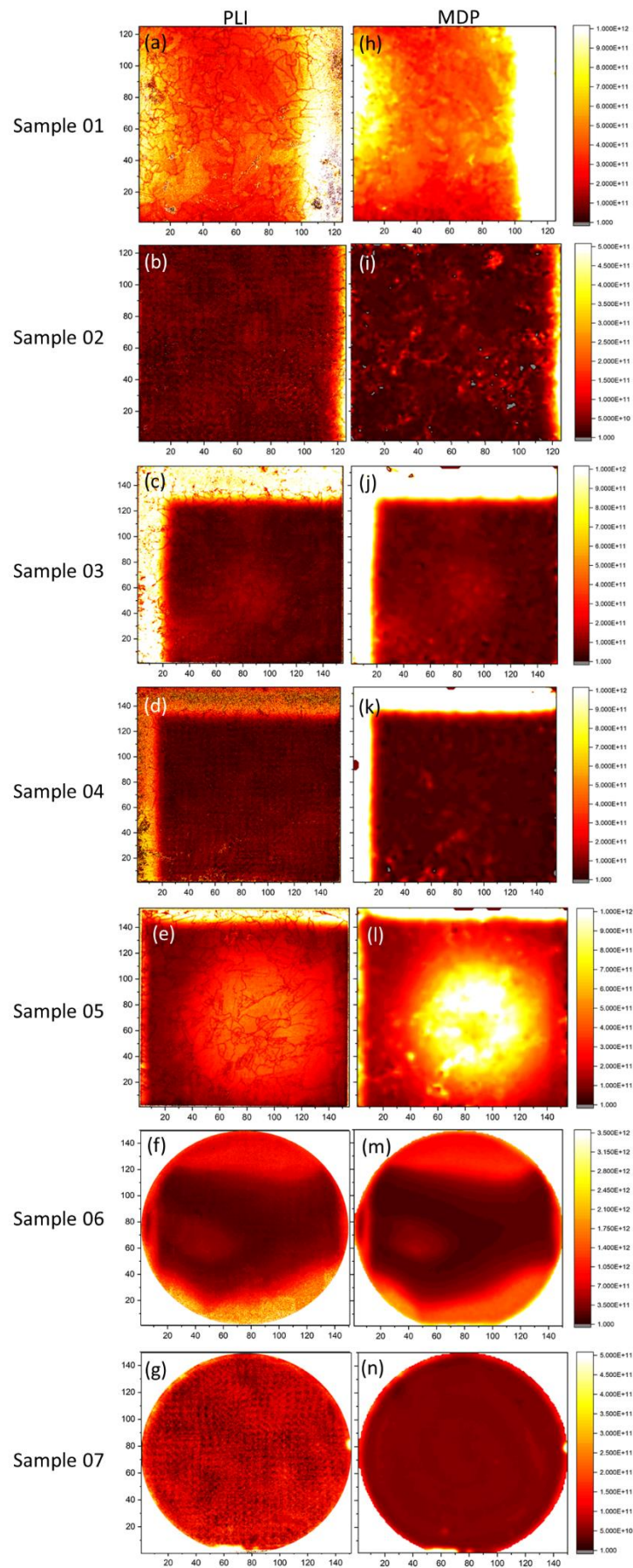


Figure 3: Fe concentration images/maps. (a) to (g) PLI Fe images and (h) to (n) MDP Fe maps.

#### 4 QUANTITATIVE COMPARISON

Fig. 4 is the quantitative Fe comparison between PLI and MDP. A good quantitative correlation of center region can be observed in Fig. 4a. Deviations in Fig. 4b are due to evaluation methods for the C factor. In PLI, evaluation is pixel to pixel considering changes in injection between FeB and Fe<sub>i</sub> states, whereas in MDP, the center region in FeB state is considered. Errors can be expected in MDP approach, as there will be changes in injection from center to edges within the same state and also from FeB to Fe<sub>i</sub> state. Due to the differences in the used defect models from MDP and PLI, at  $1 \times 10^{15} \text{cm}^{-3}$  injection one can expect a factor of 2 differences. However, the difference changes with the injections. Despite of these differences, surprisingly the factor of difference for spatially resolved comparison is maximum 2, except for one of the samples the difference is of factor 4 (Fig. 4b). This was due to very noisy image in PLI.

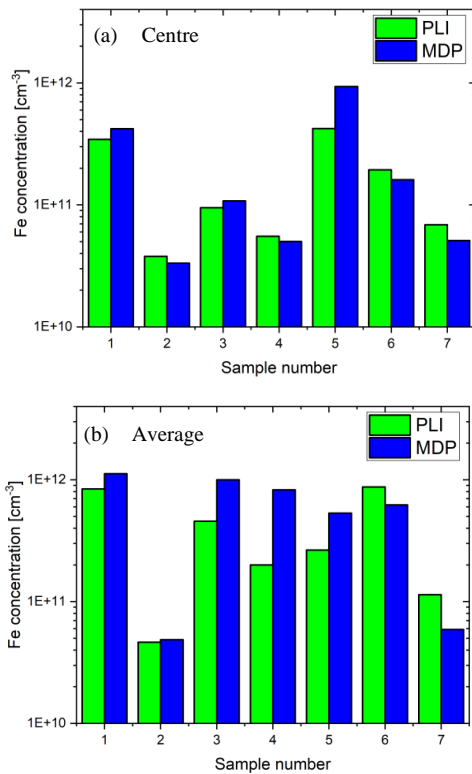


Figure 4: PLI and MDP Fe concentration comparison (a) Average in centre (b) Complete wafer.

Fig. 5 shows the quantitative comparison of all three methods. As QSSPC considers only the sensor region (40 mm circular diameter) of the stage for lifetime evaluation (i.e., centre region of wafer), from PLI and MDP images the centre region is considered for comparison with QSSPC. In Fig. 5 considering QSSPC Fe concentration on x-axis, MDP and PLI Fe concentration on y-axis depicts a good correlation.

#### 5 PROS AND CONS OF EACH METHOD

All three tools and methods are applicable for iron analysis. QSSPC offers the widest injection range, but lacks spatial resolution and requires external FeB dissociation and manual calculation. Iron analysis by PLI requires a sophisticated workflow for all the steps of

lifetime calibration and Fe-state preparation. This is not part of all commercially available PLI-Tools. MDP offers a fully automatized procedure with accurate values especially in the centre region of the wafers.

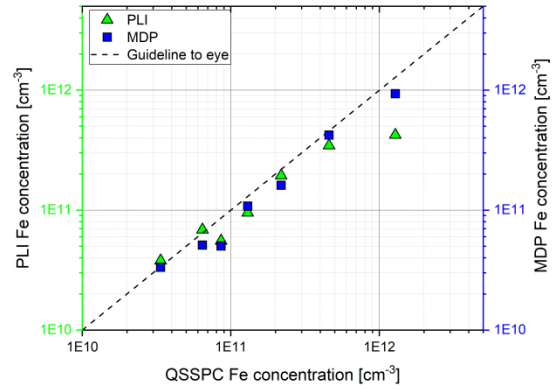


Figure 5: Comparison of three tools center regions Fe concentration.

#### 6 SUMMARY

Iron concentration detection in wafers is crucial to increase the efficiency of solar cells. In this work, iron detection tools QSSPC, PLI and MDP are compared by considering 7 samples for investigation. By storing the samples in dark for 2 days Fe-B state is prepared. As iron detection is based on change in lifetime, a comparison of three tools injection dependent lifetime measurement is performed and a good correlation is observed. Then, a good qualitative and quantitative correlation of iron concentration from three tools is reported. The centre region of wafer depicts good correlation. At the edges, differences are observed, due to different C factor evaluation methods adapted by tools.

#### 7 ACKNOWLEDGEMENT

The authors would like to thank all colleagues at the Fraunhofer ISE from the QCS department. This work was funded by the German Federal Ministry for Economic Affairs and Energy within the research projects "CUT-B" (contract no. 0325910A) and "EPI-INSPEC" (contract no. 03EE1043C).

#### REFERENCES

- [1] K. Adamczyk *et al.*, "Recombination activity of grain boundaries in high-performance multicrystalline Si during solar cell processing," *Journal of Applied Physics*, vol. 123, no. 5, p. 55705, 2018
- [2] K. Graff, *Metal Impurities in Silicon-Device Fabrication*. Berlin, Heidelberg: Springer, 2000.
- [3] E. B. Yakimov, "Metal Impurities and Gettering in Crystalline Silicon," in *Handbook of photovoltaic silicon*, D. Yang, Ed., Berlin, Germany: Springer, 2019, pp. 495–540.
- [4] A. A. Istratov, H. Hieslmair, and E. R. Weber, "Iron contamination in silicon technology," *Applied Physics A: Materials Science & Processing*, vol. 70, no. 5, pp. 489–534, 2000.

- [5] F. Schindler *et al.*, “Solar Cell Efficiency Losses Due to Impurities From the Crucible in Multicrystalline Silicon,” *IEEE J. Photovoltaics*, vol. 4, no. 1, pp. 122–129, 2014.
- [6] D. Macdonald, J. Tan, and T. Trupke, “Imaging interstitial iron concentrations in boron-doped crystalline silicon using photoluminescence,” *Journal of Applied Physics*, vol. 103, no. 7, p. 73710, 2008.
- [7] N. Schüler, S. Anger, K. Dornich, J. R. Niklas and K. Bothe, “Limitations in the accuracy of photoconductance-based lifetime measurements,” in *Solar Energy Materials & Solar Cells*, vol 98, pp. 245–252, 2012
- [8] J. A. Giesecke, M. C. Schubert, B. Michl, F. Schindler and W. Warta, “Minority carrier lifetime imaging of silicon wafers calibrated by quasi-steady-state photoluminescence” *Solar Energy Materials & Solar Cells*, vol. 95, pp. 1011–1018, 2011.
- [9] R. A. Sinton, A. Cuevas, and M. Stuckings, “Quasi-steady-state photoconductance, a new method for solar cell material and device characterization,” in *Conference Record of the Twenty fifth IEEE Photovoltaic Specialists Conference, 1996: Hyatt Regency Crystal City, Washington, D.C., May 13-17, 1996*, Washington, DC, USA, 1996, pp. 457–460.
- [10] G. Zoth and W. Bergholz, “A fast, preparation-free method to detect iron in silicon,” *Journal of Applied Physics*, vol. 67, no. 11, pp. 6764–6771, 1990.
- [11] S. Rein, and S. W. Glunz, “Electronic properties of interstitial iron and iron-boron pairs determined by means of advanced lifetime spectroscopy,” *Journal of Applied Physics*, vol. 98, no. 113711, pp.1-12, 2005.
- [12] D. H. Macdonald, L. J. Geerligs, and A. Azzizi. “Iron detection in crystalline silicon by carrier lifetime measurements for arbitrary injection and doping”, *Journal of applied physics*, 95(3):1021–1028, February 2004.